GEOPHYSICAL RESEARCH LETTERS, VOL. 26, NO. 19, PAGES 2969-2972, OCTOBER 1, 1999

Influence of the North Atlantic SST on the atmospheric circulation

Arnaud Czaja and Claude Frankignoul

Laboratoire d'océanographie Dynamique et de Climatologie (LODYC), Paris, France

Abstract. Using the monthly COADS dataset and NMC-NCAR archives we show that significant anomalies of the atmospheric circulation are related to previous SST anomalies in the North Atlantic. A signal over the northwest Labrador Sea in late spring is associated with the dominant mode of SST variability during the preceeding winter. It is more clearly seen in the mid-troposhere than at sea level and appears to be related to the anomalous surface heat exchanges that slowly damp the SST anomalies. In addition, a NAO-like signal in early winter is associated with SST anomalies east of Newfoundland and in the eastern subtropical North Atlantic during the preceeding summer.

1. Introduction

On the monthly timescale, air-sea interactions in the North Atlantic primarily reflect the stochastic forcing of the oceanic mixed-layer by the atmosphere, resulting in large-scale sea surface temperature (SST) anomalies [*Frankignoul*, 1985]. After they have been generated, the latter are damped by the turbulent surface heat flux, thereby influencing the atmospheric boundary layer [*Frankignoul et al.*, 1998]. However, the impact of the North Atlantic SST anomalies on the observed tropospheric flow has not been documented, although wintertime SST anomalies may have a small predictive skill for the winter [*Ratcliffe and Murray*, 1970] or summer [*Colman*, 1997] climatology of Northern Europe. In general, sensitivity studies with atmospheric general circulation models show that prescribed North Atlantic SST anomalies have some influence on the wintertime circulation, but the nature of the interaction is still controversial [e.g, *Kushnir and Held*, 1996]. Recently, by using an ensemble of simulations forced by the global SST and sea-ice distribution during 1948-1993, *Davies et al.* [1997], *Venzke et al.* [1998] and *Rodwell et al.* [1999], found that a significant predictability of the North Atlantic Oscillation - like mode of variability in their model was associated with SST anomalies in the North Atlantic. Further investigations of the observational records are thus needed to fill the gap with these modeling studies.

2. Data

Monthly anomalies from the mean seasonal cycle were used in the North Atlantic sector between January 1952 and December 1992. SST and turbulent surface heat flux (sensible plus latent) derived from the COADS dataset on a $5° \times 5°$ grid [*Cayan*, 1992] were considered between 20N and 60N, except in the northwest where the data density is poor. Geopotential height at 500 mb (hereafter Z500) obtained from the former NMC, and sea level pressure (hereafter SLP) and 700 mb temperature (hereafter T700) obtained from NCAR were considered between 20N to 70N and 100W to 10E. At each grid-point, a third-order polynomial was removed by least-squares fit from each anomaly time series, thereby removing the strong trends displayed in the analysis period.

3. Lead-lag analysis between SST and tropospheric variables

As reviewed in *Frankignoul* [1985], the stochastic climate model gives a good representation of extratropical SST anomalies and provides statistical signatures of their interaction with the atmosphere. The lagged covariance between SST and atmospheric anomalies is particularly revealing, as it peaks when SST lags by a few weeks and decays at longer lag with the SST anomaly decay time. Because the atmospheric forcing is basically white, the covariance is negligible when SST leads by more than the atmospheric decorrelation time if the SST anomalies have no back interaction on the atmosphere. Otherwise, there is a covariance which again decreases with increasing lead time as the SST anomaly. If the atmosphere acts as a negative (positive) feedback, the covariance changes (keeps the same) sign between negative and positive lags [*Frankignoul et al.*, 1998].

To emphasize large-scale patterns of covariability, we used a maximum covariance analysis based on a singular value decomposition of the covariance matrix between SST and atmospheric (ATM) anomalies (hereafter SVD). To give similar weight to each month and thus increase the effective number of degrees of freedom, we first normalized the anomalies in each month by their standard deviation averaged over the domain. This removes the seasonal cycle of variance, but for display we go back to dimensional fields. At each lag τ (positive when SST leads), the anomalies are decomposed into

$$SST(x,t) = \sum_k u_k(x,\tau) s_k(t,\tau) \qquad (1)$$

$$ATM(x,t+\tau) = \sum_k v_k(x,\tau) z_k(t+\tau,\tau) \qquad (2)$$

where the time series s_k and z_k have maximum covariance for each k, under the constraint that the spatial patterns u_k and v_k form sets of orthonormal vectors [*Bretherton et al.*, 1992]. As evidence of an oceanic influence turned out to be strongest when using the late winter (February-March-April,

Paper number 1999GL900613.
0094/8276/99/1999GL900613$05.00

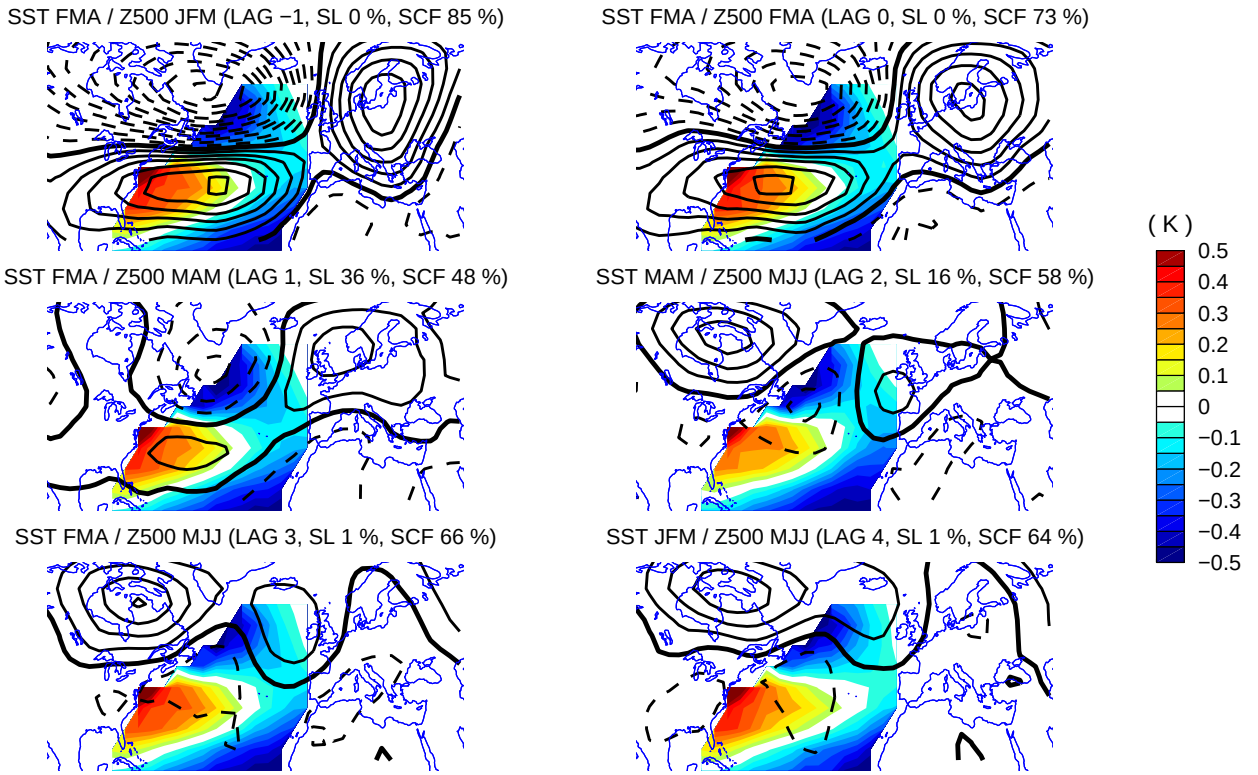

Plate 1. SVD of Z500 (contour 5 m, negative values are dashed) and winter SST anomalies (color scale in K). The months used to define the lags, the significance level (SL) and the squared covariance fraction (SCF) explained by the mode are indicated. The Z500 patterns have been extended westward and eastward by linear regression.

hereafter FMA) and late summer (July-August-September, hereafter JAS) SST anomalies, we only discuss these two cases. Note that we work with monthly anomalies, not seasonal ones. Only the first mode ($k = 1$) is considered, as the next ones are increasingly sensitive to sampling fluctuations. Scaled homogeneous covariance maps for SST and heterogeneous covariance ones for ATM, i.e, the projection of both fields on the (normalized) time series $s_1(t, \tau)$ preserve linear relations between them and are used for display. For each lag, statistical significance of the squared covariance $< s_1(t,\tau)z_1(t+\tau,\tau) >^2$ is assessed with a Monte Carlo approach, randomly permuting the years but not the months of the ATM sequence, with a minimum separation of 2 yr between SST and ATM anomalies (100 realizations). The estimated significance level is the percentage of randomized squared covariances for the first mode that exceeds the squared covariance being tested.

During winter, the largest squared covariances are found at lags ≤ 0, reflecting the SST anomaly response to the stochastic atmospheric forcing. The Z500-pattern (Plate 1)

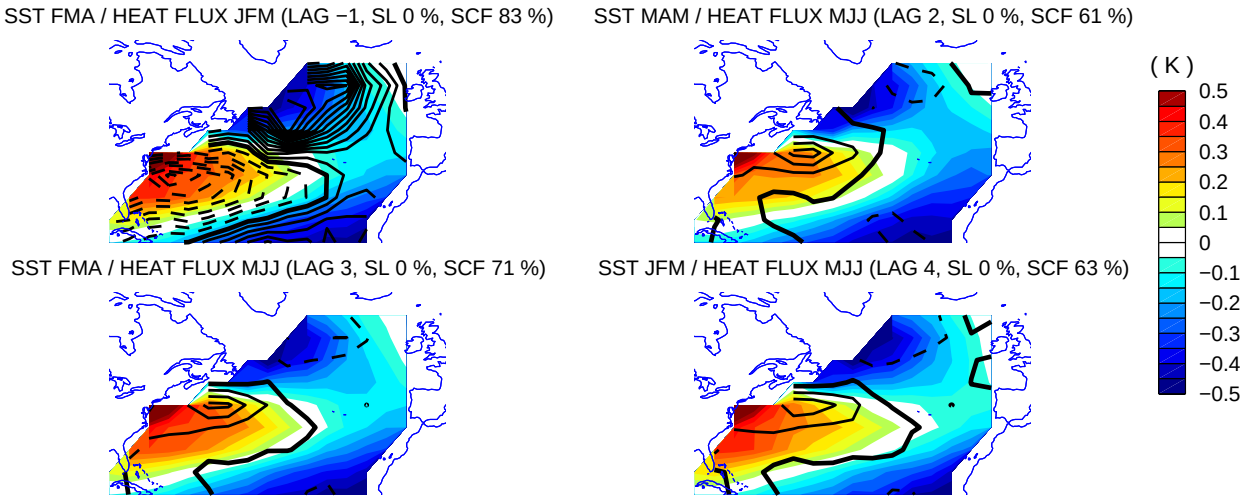

Plate 2. As in Plate 1 but for the surface turbulent heat flux (positive upward, contour 3 Wm^{-2}) instead of Z500. Lag 0 and 1 are not represented.

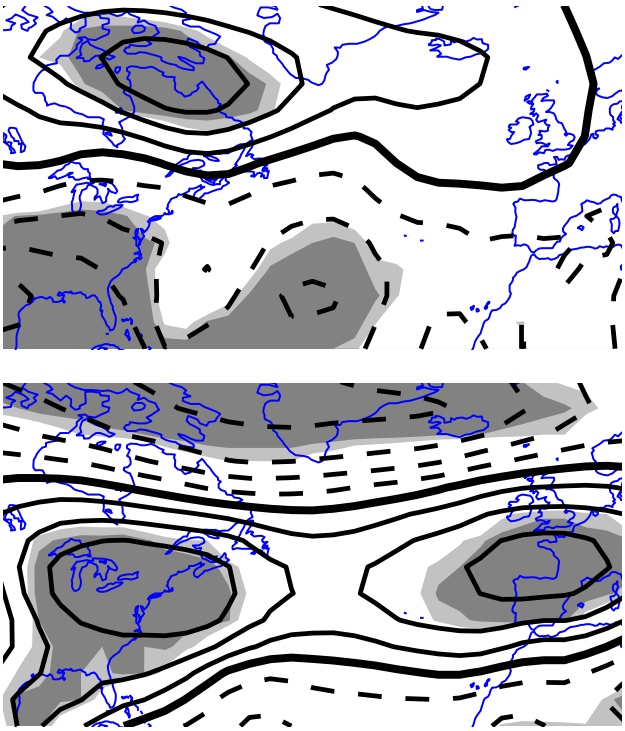

Figure 1. Correlation maps of Z500 with the SVD time series of SST at lag 4 (contour 0.1, negative contours dashed) for winter (top) and summer SST. The dark and light shading denotes respectively where the correlation is significant at the 5% and 10% level, as deduced from Monte Carlo simulations.

is similar to the Western Atlantic pattern of *Wallace and Gutzler* [1981], which primarily generates SST fluctuations via turbulent heat exchanges (Plate 2). The SST tripole pattern is almost identical to the first empirical orthogonal function of SST in late winter (hereafter SST1), persisting for more than 3 months. Similar patterns are found at lag 1 because of the small persistence of the atmosphere, but the squared covariance is much smaller and not significant. When the ocean leads by more than one month, however, the squared covariance increases again and becomes significant until lag 6 when significance is lost. The SST pattern is similar to that when the atmosphere leads, but not the Z500 one which now has a center of action west of the Labrador Sea. Anomalous anticyclonic circulation above the Labrador Sea in late spring - early summer is thus associated with SST1 at the end of the previous winter (warmer subtropical gyre, colder subpolar gyre). The relation is robust and the associated squared covariance fraction about 60 % (Plate 1). Although the mode only represents a small fraction of the total Z500 variance (e.g., 14 % at lag 3), it locally explains a substantial fraction (75 % above the Labrador sea). Local significance of the Z500 pattern can be estimated by comparing the heterogeneous correlation maps for Z500 with that of the Monte Carlo simulations. It is high above the Labrador Sea and the western subtropic, as illustrated in Figure 1 (top). A significant signal with a similar pattern of the same sign is also found in the lagged SVD with T700, suggesting that the tropospheric perturbation is equivalent barotropic (not shown). Although the pattern is also seen with SLP, statistical significance is lost.

The lagged SVD with the surface heat flux (Plate 2) suggests that the anomalous tropospheric circulation may be driven in part by the heat exchanges associated with the SST anomaly. Indeed, the turbulent heat flux anomaly changes sign between positive and negative lags while keeping roughly the same pattern, so that it acts as a negative feedback on the SST anomaly which then anomalously heats or cools the atmosphere. At lag 2, a $0.4^{\circ}C$ SST anomaly is associated with a 6 Wm^{-2} heat flux anomaly 2 months later. Since the SST anomaly decreases by a factor $\sqrt{2}$ in 2 months, the negative feedback is of order $6/(0.4/\sqrt{2}) \simeq 20\ Wm^{-2}K^{-1}$, which agrees with *Frankignoul et al.* [1998]. Using a similar reasoning, the associated Z500 perturbation would be $\simeq 40\ mK^{-1}$. However these values may be overestimated since they are based on maximized covariances. Furthermore, if the relation between SST and surface heat flux in lead and lag conditions is consistent with the stochastic model, that with Z500 is somewhat different. The stochastic model predicts that a SST influence should be most easily detectable at lag 2, as lag 1 (but not lag 2) is obscured by the persistence of Z500 (i.e. lag 1 reflects both the forcing of and response to SST). However,

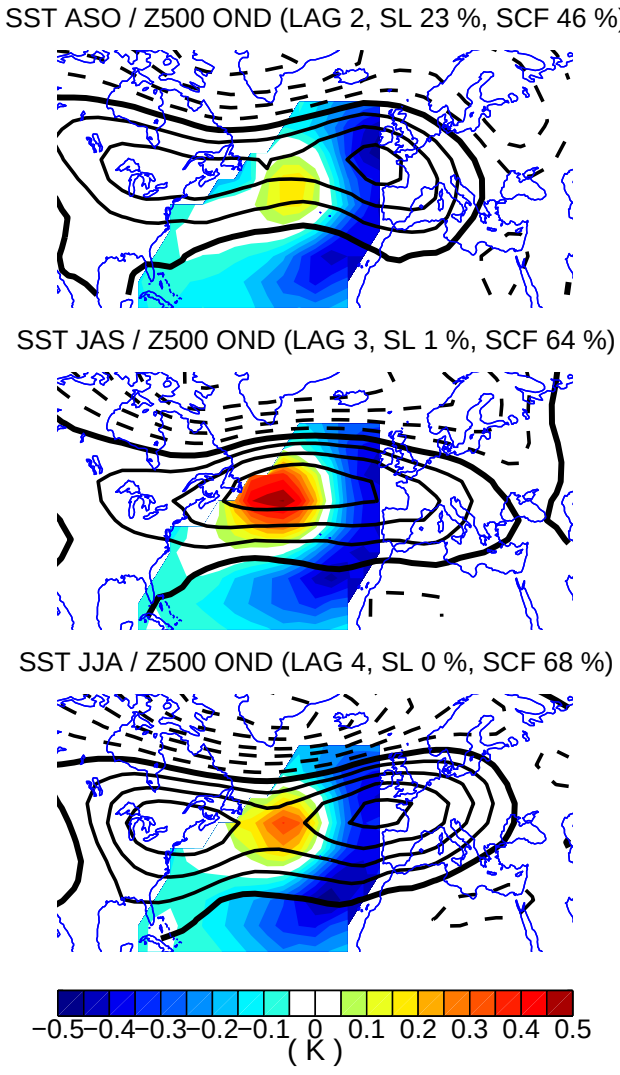

Plate 3. As Plate 1 but for summer SST anomalies.

the squared covariance peaks at lag 3 and 4, suggesting more complex dynamics, as discussed below.

When considering the late summer SST anomalies, the largest squared covariances between SST and Z500 are also found at lags ≤ 0, but the turbulent heat flux plays a lesser role in generating the summer SST anomalies (not shown). A strong evidence of an oceanic influence on the atmosphere is again found at lag ≥ 2 (Plate 3). A dipolar tropospheric anomaly reminiscent of the positive (negative) phase of the North Atlantic Oscillation (hereafter NAO) is associated in early winter with a cooler (warmer) SST in the northeast Atlantic and a warmer (colder) SST east of New Foundland during the preceeding summer. A similar and equally significant anomaly is found in SLP and T700 where it is shifted slightly westward (not shown). The squared covariance is highly significant between lag 3 and 6, decaying thereafter. As in the previous case, the mode represents about 60 % of the squared covariance, but it explains a larger fraction of the total variance (25 % of Z500 at lag 3). As shown in Fig. 1 (bottom), both the low and high pressure bands of the Z500 patterns in Plate 3 are locally significant. Although we found a sign reversal of the heat flux pattern between lag -1 and 1 (not shown), the signal is less clear at larger lags and the negative heat flux feedback seems to only play a small role in the summer case. Note that these results differ from the modelling one of *Rodwell et al.* [1999], who associated a NAO-like response to SST1 instead of the SST pattern in Plate 3. Also, they were only considering the atmospheric response in winter (DJF).

4. Discussion

Our analysis reveals statistically significant lagged relationships between large-scale SST and subsequent midtropospheric anomalies in the North Atlantic sector during two different seasons. In both cases, we find that the tropospheric signal is maximum when the SST leads the atmosphere by 3 to 5 months, whereas a simple stochastic climate model would predict that the maximum is found at lag 2. Colman [1997] similarly found a gap in predictive skill at a lead time of 2 months. The prevalence of longer lags than predicted may result from the seasonal dependence of the atmospheric response to a given SST anomaly pattern. As the latter persists for several months, it underlies a changing atmospheric background flow which may be insensitive to a SST pattern at the time when it has generated it, but strongly respond when the tropospheric flow has changed. Alternatively, the shift towards longer lags could be due to the influence of other regions which were not included in our analysis but could play an important role via teleconnections. By extending the correlations in Fig.1 to the global SST field, we found that SST anomalies in the tropical Atlantic (but not the tropical Pacific) were also associated with the SST patterns in Plate 1 to 3. As the atmosphere is more persistent in the tropics, the lag 2 covariances may also be perturbed by a small influence of the forcing patterns. In late spring, the anomalous tropospheric circulation over the western Labrador Sea might also be related to sea ice extent anomalies. A more extended analysis aiming at understanding the respective role of the low and high latitudes in the SST influence revealed here is underway, using the NCEP reanalysis.

Acknowledgments. We thank D. Cayan, Scripps Institution of Oceanography, for kindly providing the heat flux and SST data, and the referees for their useful comments. This research was supported in part by EEC Grant ENV4-CT98-0714.

References

Bretherton, C. S., and C. S. Smith, and J. M. Wallace, An intercomparison of methods for finding coupled patterns in climate data, *J. Climate*, *5*, 541-560, 1992.

Cayan, D., Latent and sensible heat flux anomalies over the Northern oceans: driving the sea surface temperature, *J. Phys. Oceanogr.*, *22*, 859-881, 1992.

Colman, A., Prediction of summer central England temperature from preceding North Atlantic winter sea surface temperature, *Int. J. Clim.*, *17*, 1285-1300, 1997.

Davies, J. R., and D. P. Rowell, and C. K. Folland, North Atlantic and European seasonal predictability using an ensemble of multidecadal AGCM simulations, *Int. J. Clim.*, *17*, 1263-1284, 1997.

Frankignoul, C., Sea surface temperature anomalies, planetary waves and air-sea feedbacks in the middle latitude, *Rev. of Geophys.*, *23*, 357-390, 1985.

Frankignoul, C. and A. Czaja and B. L'Hévéder, Air-sea feedback in the North Atlantic and surface boundary conditions for ocean models, *J. Climate*, *11*, 2310-2324, 1998.

Kushnir, Y. and I. Held, Equilibrium atmospheric responses to North Atlantic SST anomalies, *J. Climate*, *9*, 1208-1220, 1996.

Ratcliffe, R. A., and R. Murray, New lag associations between North Atlantic sea temperature and european pressure applied to long-range weather forecasting, *Quart. J. Roy. Meteor. Soc.*, *96*, 226-246, 1970.

Rodwell, M. J., D. P. Rowell, and C. K. Folland, Oceanic forcing of the wintertime North Atlantic Oscillation and Europeean climate, *Nature*, *398*, 320-323, 1999.

Wallace, J. M., and D. S. Gutzler, Teleconnections in the geopotential height field during the Northern hemisphere winter, *Monthly Weather Rev.*, *109*, 784-812, 1981.

A. Czaja and C. Frankignoul Laboratoire d'océanographie Dynamique et de Climatologie (LODYC, T15), 4 Place Jussieu 75 005 Paris, France. (e-mail acz@lodyc.jussieu.fr)

(Received April 15, 1999; revised June 16, 1999;
accepted June 18, 1999.)